Sorting receptor Rer1 controls surface expression of muscle acetylcholine receptors by ER retention of unassembled α-subunits

Christina Valkova[a,1], Marina Albrizio[b,1], Ira V. Röder[b], Michael Schwake[c], Romeo Betto[d], Rüdiger Rudolf[b,2], and Christoph Kaether[a,2]

[a]Leibniz Institut für Altersforschung-Fritz Lipmann Institut, 07743 Jena, Germany; [b]Institut für Toxikologie und Genetik, Karlsruhe Institute of Technology, 76021 Karlsruhe, Germany; [c]Biochemisches Institut, Christian-Albrechts-Universität Kiel, 24098 Kiel, Germany; and [d]Consiglio Nazionale delle Ricerche Istituto di Neuroscienze, Università di Padova, 35121 Padua, Italy

Edited* by Jennifer Lippincott-Schwartz, National Institutes of Health, Bethesda, MD, and approved December 6, 2010 (received for review February 14, 2010)

The nicotinic acetylcholine receptor of skeletal muscle is composed of five subunits that are assembled in a stepwise manner. Quality control mechanisms ensure that only fully assembled receptors reach the cell surface. Here, we show that Rer1, a putative Golgi-ER retrieval receptor, is involved in the biogenesis of acetylcholine receptors. Rer1 is expressed in the early secretory pathway in the myoblast line C2C12 and in mouse skeletal muscle, and up-regulated during myogenesis. Upon down-regulation of Rer1 in C2C12 cells, unassembled acetylcholine receptor α-subunits escape from the ER and are transported to the plasma membrane and lysosomes, where they are degraded. As a result, the amount of fully assembled receptor at the cell surface is reduced. In vivo Rer1 knockdown and genetic inactivation of one Rer1 allele lead to significantly smaller neuromuscular junctions in mice. Our data show that Rer1 is a functionally important unique factor that controls surface expression of muscle acetylcholine receptors by localizing unassembled α-subunits to the early secretory pathway.

protein complex | protein transport | retention/retrieval

Induction of muscle contraction is mediated by acetylcholine release from the motor neuron at the neuromuscular junction (NMJ). On the muscle, this signal is decoded by the nicotinic acetylcholine receptor (AChR). The AChR is a pentameric ion channel composed of two α-subunits, one β-, one δ-, and a γ- (embryonic/regenerating) or an ε- (adult) subunit (for review, see ref. 1). AChRs are targets of autoimmune antibodies leading to Myasthenia gravis (2), and mutations in AChR subunits can lead to congenital myasthenic syndromes (3).

AChR subunits are polytopic membrane proteins that are synthesized in the ER, where also the assembly of the complex takes place (4). As part of a quality control, specific ER-retention/retrieval signals ensure that unassembled subunits are prevented from reaching the cell surface (for review, see ref. 5). Little is known about the components of this quality control. Rer1 is a unique sorting receptor involved in ER retention/retrieval of unassembled subunits of large oligomeric membrane protein complexes, for example, the yeast iron transporter (6). Like the KDEL receptor (KDELR), Rer1 is localized in early secretory compartments, mainly the *cis*-Golgi (7). Recently, mammalian Rer1 was shown to be involved in retaining/retrieving unassembled Pen2 (8) and Nicastrin (9), both membrane protein constituents of the γ-secretase, to the ER. Here, we provide in vitro and in vivo evidence that Rer1 blocks the surface exposure of unassembled AChRα subunits and that reduced expression of Rer1 affects the size of neuromuscular synapses.

Results

Rer1 Is Expressed in Muscle and Up-Regulated During Myogenesis. To evaluate a possible involvement of Rer1 in muscle AChR assembly, we first characterized the expression of endogenous Rer1 in mouse skeletal muscle. Western blot analysis showed that Rer1 is present in all tested muscle types (Fig. 1*A*). Next, we addressed the localization of endogenous Rer1 in the myoblast line C2C12, which can be differentiated into myotubes upon serum withdrawal (10). Subcellular fractionation (Fig. 1*B*) and cell surface biotinylation (Fig. S1) demonstrated that Rer1 localizes to the early secretory pathway, mostly the ER-Golgi intermediate compartment (ERGIC). This finding was corroborated by immunohistochemical colocalization analysis in skeletal muscle (Fig. S1), and it is consistent with previous findings in other cell types (7, 8). In C2C12 cells, Rer1 expression increased strongly during differentiation, concomitant with the up-regulation of AChRα (Fig. 1 *C* and *D*). This augmentation did not simply reflect an enlargement of the secretory pathway upon differentiation, because GM130 and ERGIC53, markers for the *cis*-Golgi and the ERGIC, respectively, were not, or only slightly, up-regulated (Fig. 1*C*). Taken together, these data suggest that Rer1 plays a role in AChR biogenesis.

Rer1 Controls Surface Exposure of AChRα in Vitro. To characterize a potential role of Rer1 in AChR surface exposure, we used C2C12 cells as an established model system. Efficient siRNA-mediated knockdown of Rer1 led to decreased AChRα levels at the plasma membrane (PM), as measured by surface labeling with biotin-αBungarotoxin (αBT) (Fig. 2*A*). As a control, γ-sarcoglycan, a component of a heterooligomeric complex of the muscle PM (11), remained unaffected after Rer1 knockdown (Fig. 2*A*). This observation demonstrated that reduction of Rer1 did not affect general assembly/transport mechanisms. Quantitation in Rer1 siRNA-transfected C2C12 cells revealed a significant reduction in both the ratio of surface to total AChRα and the total levels of AChRα as compared with control cells (Fig. 2 *B* and *C*). These changes were due neither to a transcriptional down-regulation of AChRα nor to a delay in differentiation (Fig. S2). Although AChRβ could not be assessed because appropriate antibodies were lacking, AChRγ/δ were not affected by Rer1 knockdown, suggesting that Rer1 interacts specifically with AChRα (Fig. S2). These data suggest that Rer1 controls the surface expression of AChRα in vitro.

Rer1 Directly Binds to Unassembled AChRα. Next, we tested whether Rer1 directly interacts with AChRα. Immunoprecipitation with

Author contributions: R.B., R.R., and C.K. designed research; C.V., M.A., I.V.R., and M.S. performed research; R.B. contributed new reagents/analytic tools; C.V., M.A., R.R., and C.K. analyzed data; and R.R. and C.K. wrote the paper.

The authors declare no conflict of interest.

*This Direct Submission article had a prearranged editor.

[1]C.V. and M.A. contributed equally to this work.

[2]To whom correspondence may be addressed. E-mail: ckaether@fli-leibniz.de or ruediger.rudolf@kit.edu.

This article contains supporting information online at www.pnas.org/lookup/suppl/doi:10.1073/pnas.1001624108/-/DCSupplemental.

CELL BIOLOGY

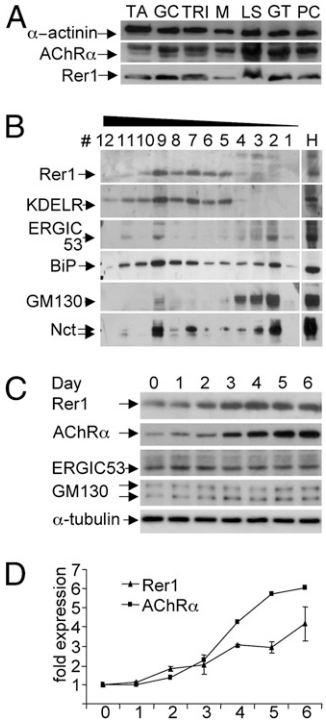

Fig. 1. Rer1 is expressed in skeletal muscle and up-regulated during myogenesis. (*A*) Lysates from different muscles were prepared from a 2-mo-old mouse, separated on SDS/PAGE and blotted by using antibodies against α-actinin, AChRα, and Rer1. Muscles tested were TA, tibialis anterior; GC, gastrocnemius; TRI, triceps surae; M, masseter; LS, longissimus dorsae; GT, gluteus; and PC, pectoralis. (*B*) Subcellular fractionation of differentiated C2C12 cells was performed by discontinuous Optiprep gradient centrifugation. Fractions of decreasing density were harvested and subjected to SDS/PAGE followed by Western blotting with indicated antibodies. Rer1 distributes over the gradient very similar to the KDEL receptor with a peak in fraction 9 were also ERGIC53 and BIP concentrate. (*C*) C2C12 cells were differentiated for 6 d by serum withdrawal. Cell lysates harvested at indicated time points were probed for indicated antibodies (α-tubulin, loading control). (*D*) Quantitation of relative expression levels of Rer1 and AChRα of $n = 3$ independent experiments is shown. Rer1 and AChRα expression levels at day 0 were set to 1.

Rer1 antibody or IgG control, and subsequent blotting for AChRα, revealed that only the Rer1-specific antibody precipitated AChRα, suggesting a direct interaction between the two proteins (Fig. 3*A*). Conversely, AChRγ/δ subunits did not coprecipitate with Rer1 at detectable amounts (Fig. 3*A*). However, the signal in the lysate was too weak to allow a definite conclusion. Notably, AChRα was found to coprecipitate only with Rer1 but not with another Golgi-localized membrane protein, the KDELR, underscoring the specificity of the coimmunoprecipitation (Fig. 3*B*). Furthermore, we found that Rer1 interacts with intracellular AChRα molecules, because similar amounts of the subunit coimmunoprecipitated with Rer1 before and after depletion of the surface AChRα (Fig. 3*C*). These data suggest that, in line with its localization in early secretory compartments, Rer1 interacts with intracellular, unassembled AChRα. The low amount of AChRα bound to Rer1 is consistent with only a small fraction of receptor subunits being retrieved at steady state.

Rer1 Retains/Retrieves Unassembled AChRα. To understand in more detail the effect of Rer1 down-regulation, the assembly status of AChRα at the PM of C2C12 cells was assessed. Therefore, we determined the ratio of assembled to unassembled AChRα at the PM by means of binding of αBT to AChRα with or without preincubation with carbachol. Whereas αBT binds both assembled and unassembled AChRα subunits, carbachol only binds to assembled AChRs and blocks the binding site for αBT, thus allowing us to determine the ratio of assembled to unassembled AChRs (12). As expected, in cells transfected with control siRNA, most of the AChRα at the PM was assembled into AChRs (Fig. 4*A*). In cells transfected with Rer1 siRNA, the total amount of assembled plus unassembled AChRα at the PM was

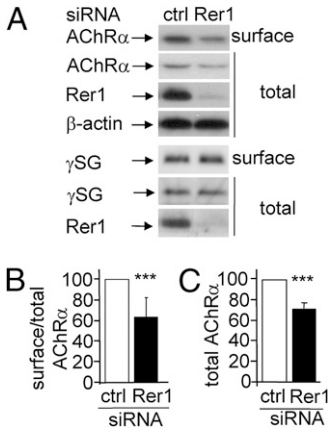

Fig. 2. Rer1 knockdown leads to reduced AChR expression at the plasma membrane in vitro. (*A*) C2C12 cells were electroporated with control (ctrl) or Rer1 siRNA, differentiated for 5 d, and then subjected to surface labeling with αBT-biotin for AChRα and surface biotinylation for γ-sarcoglycan (γ-SG). Streptavidin precipitates (surface) and total lysates were separated by SDS/PAGE and probed for indicated proteins. (*B* and *C*) Quantitation of the surface to total AChRα ratio (*B*) and of total AChRα levels (*C*) in control (100%) and Rer1 siRNA-transfected cells from $n = 5$ independent experiments. Error bars, SEM; $^{***}P \leq 0.001$.

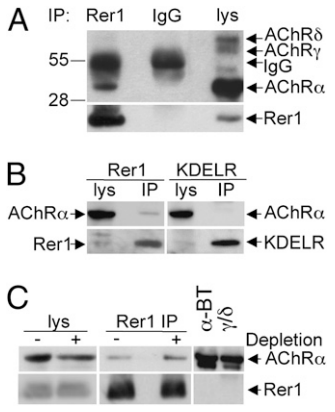

Fig. 3. Rer1 binds to intracellular unassembled AChRα. (*A*) Coimmunoprecipitation of Rer1 and AChRα. STEN lysates from C2C12 cells were immunoprecipitated with anti-Rer1 antibody or IgG, separated on SDS/PAGE, and probed for indicated proteins. Molecular mass markers (kilodaltons) are shown on the left side. (*B*) AChRα coimmunoprecipitates with Rer1 but not with KDELR. CHAPSO lysates from differentiated C2C12 cells were immunoprecipitated with anti-Rer1 or with anti-KDELR antibody (indicated on top), separated on SDS/PAGE, and probed for AChRα and Rer1 or KDELR (indicated with arrows). (*C*) Similar amounts of AChRα coprecipitate with Rer1 before and after depletion of the surface receptor. Differentiated C2C12 cells were surface labeled with α-BT-biotin. STEN lysate (– depletion) and the supernatant after streptavidin precipitation (+ depletion) were immunoprecipitated with Rer1 antibody, separated on SDS/PAGE, and probed for Rer1 and AChRα. For comparison, streptavidin precipitation of surface-labeled AChRα and coimmunoprecipitation with antibodies against AChRγ/δ are shown. In *B* and *C*, Rer1 antibody covalently coupled to beads was used.

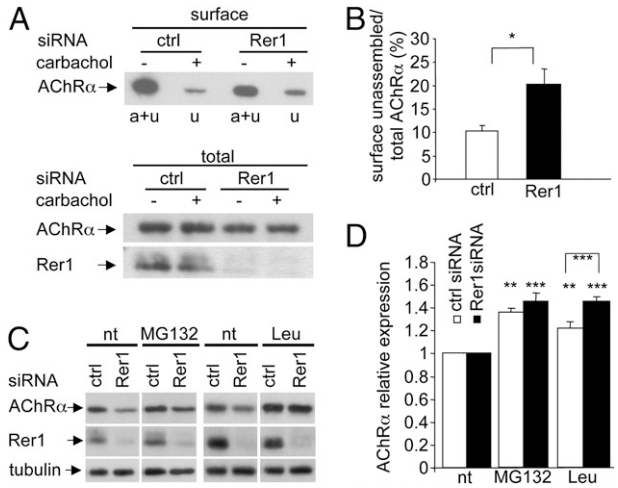

Fig. 4. Rer1 retains/retrieves unassembled AChRα and prevents it from degradation in lysosomes. (*A*) C2C12 cells were electroporated with control (ctrl) or Rer1 siRNA, differentiated for 4 d and surface-labeled with αBT-biotin with or without preincubation with carbachol. Streptavidin precipitates and lysates were separated on SDS/PAGE, and Western blots were probed with indicated antibodies. a, assembled; u, unassembled. (*B*) Quantitation from $n = 5$ independent experiments as in *A*. Ratios of unassembled and total AChRα at the PM were determined with chemiluminescence. Error bars, SEM; $*P < 0.05$. (C) C2C12 cells were electroporated with control (ctrl) or Rer1 siRNA, differentiated for 5 d, incubated with vehicle, MG132 or leupeptin (Leu), subjected to Western blot, and probed with indicated antibodies. (*D*) Quantitation from $n = 4$ independent experiments as shown in *C*. Relative expression levels of AChRα were determined with chemiluminescence. Note that relative AChRα levels are displayed; absolute levels are reduced in the absence of Rer1, see also Fig. 2*C*. Error bars, SEM; $**P < 0.01$; $***P < 0.001$.

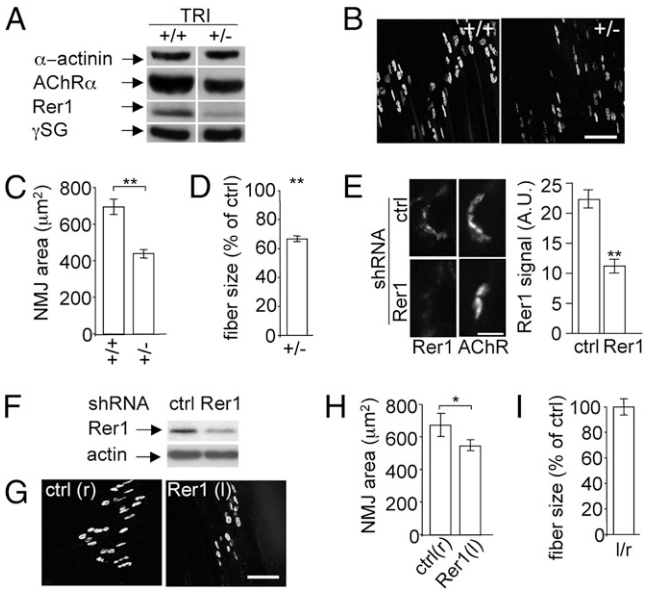

Fig. 5. Alteration of Rer1 expression modifies NMJ size in vivo. (*A*) Triceps (TRI) from $Rer1^{+/+}$ ($^{+/+}$) and $Rer1^{+/\beta\text{-geo}}$ ($^{+/-}$) littermates were lysed, and Western blotting with indicated antibodies was performed. α-actinin serves as loading control. (*B*) Tibialis anterior muscles of $Rer1^{+/+}$ ($^{+/+}$) and $Rer1^{+/\beta\text{-geo}}$ ($^{+/-}$) littermates were injected with αBT-AF647 and then monitored with in vivo confocal microscopy. (Scale bar: 200 μm.) (*C*) Quantitation of NMJ sizes as defined by αBT-AF647 staining. Shown are mean values of $n = 3$ different litters ± SEM. At least 200 NMJs per condition were quantified. Significance was tested by using Welch test ($**\alpha \leq 0.01$). (*D*) Quantitation of fiber diameter reduction. Shown are mean values from $n = 3$ different litters ± SEM. At least 700 fibers were analyzed per condition. Values from $Rer1^{+/+}$ mice were set to 100%, and values from $Rer1^{+/\beta\text{-geo}}$ ($^{+/-}$) littermates related to them. Significance was tested by using Welch test ($**\alpha \leq 0.01$). (*E Left*) Tibialis anterior muscles of WT mice were transfected with Rer1 pSilencer (left leg, Rer1) or cytoplasmic Venus (right leg, ctrl). Ten days later, they were dissected, sectioned, and stained with anti-Rer1 antibodies and αBT-AlexaFluor647 and monitored by confocal microscopy. (Scale bar: 10 μm.) (*E Right*) The graph shows the mean reduction in Rer1 fluorescence in 70 NMJs from $n = 3$ littermates per condition. (*F*) C2C12 cells were transfected with control (ctrl) or Rer1 pSilencer. After 4 d, lysates were separated on SDS/PAGE and membranes were probed with indicated antibodies. (*G*) Tibialis anterior muscles of WT mice were transfected with Rer1 pSilencer (left leg) or cytoplasmic Venus (right leg, control). Ten days later, they were injected with αBT-AF647 and then monitored with in vivo confocal microscopy. (Scale bar: 200 μm.) (*H*) Quantitation of NMJ sizes. Shown are mean values of $n = 6$ animals ± SEM. At least 380 NMJs per condition were quantified. Significance was tested by paired Student's *t* test ($*\alpha \leq 0.05$). (*I*) Quantitation of fiber diameter reduction. Shown are mean values from $n = 4$ animals ± SEM. At least 330 fibers were analyzed per condition. Values from right legs (control) were set to 100%, and values from left legs (Rer1 knockdown) related to them. Significance was tested by paired Student's *t* test.

reduced (Fig. 4*A*). Additionally, a significantly higher fraction of AChRα was unassembled (20% versus 10% in control treated cells; Fig. 4 *A* and *B*). Thus, a lack of Rer1 led to the escape of unassembled subunits out of the ER to the PM, explaining the change in the ratio of assembled/unassembled AChRα at the PM. To analyze why the total levels of AChRα were reduced in Rer1 down-regulated cells, AChRα levels were assayed upon blockage of proteasomal and lysosomal degradation. In control cells, both inhibition of the proteasome with MG132 or of lysosomal degradation with leupeptin resulted in an increase in total AChRα levels, as observed (13, 14) (Fig. 4 *C* and *D*). In the case of MG132 treatment, Rer1 down-regulation further slightly increased these levels, but the effect was not significant. In contrast, in cells with reduced Rer1 levels, leupeptin treatment significantly enhanced AChRα levels above those of cells with normal Rer1 levels (Fig. 4 *C* and *D*). Together, these data imply that Rer1 is not involved in ER-associated degradation of AChRs. Instead, in the absence of Rer1, AChRα escapes from the ER and is then degraded in lysosomes. Therefore, this degradation route could be responsible for the reduction in total AChRα levels observed in C2C12 cells with Rer1 knockdown.

Rer1 Controls Total Amount and Surface Exposure of AChR in Vivo. To reveal a functional role of Rer1 in vivo, we analyzed AChRs in mouse NMJs under different experimental conditions in which Rer1 was down-regulated. First, we used Rer1 gene-trap mice, which harbor a β-*geo* gene followed by a stop codon in the Rer1 locus (Fig. S3). Notably, Rer1 and AChRα, but not γ-sarcoglycan, levels were significantly reduced in muscles derived from $Rer1^{+/\beta\text{-geo}}$ mice compared with WT littermates (Fig. 5*A*), confirming in vivo the role of Rer1 on AChRα levels as found in C2C12 cells (Fig. 2*C*). Analysis of NMJs by in vivo confocal microscopy of muscles from $Rer1^{+/\beta\text{-geo}}$ mice injected with fluorescent αBT-AlexaFluor647 revealed a relatively inconspicuous morphology of synapses (Fig. 5*B*). However, quantitative comparison of NMJs from $Rer1^{+/\beta\text{-geo}}$ mice with those of WT littermates showed a highly significant reduction of NMJ sizes in heterozygotes (Fig. 5*C*). Because in these mice the fiber diameters also were smaller (Fig. 5*D*) and NMJ size was found to correlate with fiber diameter (15), this result did not clarify whether the NMJ shrinkage was primary to the changes in fiber morphology. To address this issue, Rer1 expression was acutely knocked down in WT mice by using in vivo transfection of shRNA. Rer1 immunoreactivity was clearly reduced in transfected fibers (Fig. 5*E*). Because transfection was restricted to superficial fiber layers and, therefore, the amount of Rer1 in the whole muscle was not sufficiently reduced to see differences in Western blot, C2C12 cells were used to confirm the efficacy of the shRNA (Fig. 5*F*).

In vivo imaging (Fig. 5*G*) revealed that NMJs were significantly smaller after 10 d of transfection with Rer1 shRNA as compared with control muscles (Fig. 5*H*). Importantly, fiber diameters remained unaltered under these conditions (Fig. 5*I*), showing that NMJ shrinkage was not due to changes in fiber caliber. These data suggest that Rer1 controls the amount of AChRs at the surface and, hence, NMJ size.

Discussion

Despite its prime importance in health and disease, little is known about the mechanisms and molecules that guide the assembly of mammalian skeletal muscle AChR in the ER. Newly synthesized subunits interact with the general folding machinery including calnexin and BIP (16). In *Caenorhabditis elegans*, three genes are essential for functional reconstitution of the levamisole-sensitive AChR (L-AChR) (17). One of them, UNC-50, is important for forward trafficking (18). Recently, the *C. elegans* proteins NRA-2 and NRA-4 were shown to regulate subtype composition in L-AChR (19). Whether their mammalian orthologs have similar functions is not known. In mammals, the ER-chaperone RIC-3 is involved in the assembly of some neuronal AChR subtypes, but a role in skeletal muscle has not been clearly established (20). We show here that Rer1, a putative Golgi-ER-retrieval receptor, controls the amount of AChRs at the PM, presumably by retaining/retrieving unassembled AChRα to the ER (for a model, see Fig. S4). Loss of Rer1 results in escape of unassembled AChRα subunits, which then have different destinations: accumulation at the PM and degradation in lysosomes. Maybe also ER-associated degradation plays a role. Escaped AChRα is unavailable for assembly into AChRs, resulting in a reduction of fully assembled, cell surface-localized AChRs. In vivo this sequence of events leads to a reduced NMJ size. Is Rer1 interacting with unassembled β-, δ-, and γ/ε subunits? AChRγ/δ protein levels are not affected after Rer1 knockdown and AChRγ/δ is not detectable in coimmunoprecipitates with Rer1, but a thorough analysis is hampered because tools like carbachol and αBT, both of which are specific for the α-subunit, are lacking.

In conclusion, our results support the idea that the early secretory pathway is very important in controlling the amount of AChR at the PM. We identified Rer1 as a unique factor determining the levels of AChR at the PM and, thus, NMJ size. It will be interesting to investigate in skeletal muscle potential interactions of Rer1 with other factors like RIC-3 and to investigate the role of Rer1 in aged or myopathic muscles, both conditions that are characterized by loss of AChRs.

Materials and Methods

Antibodies, Fluorescent Probes, and Cell Lines. For a list of antibodies used, see *SI Materials and Methods*. C2C12 cells were grown in DMEM supplemented with 10% FCS. For differentiation, cells were plated at a density of 6×10^4 cells/cm^2 and starved in DMEM with 1% FCS.

cDNA Constructs, siRNA, and Transfections. In vivo transfection of mouse tibialis anterior muscles was performed as described (21) by using the following constructs: pSilencer2.1-U6 puro with the Rer1 target sequence GAGGCAAATCAAGCACATG and cytoplasmic Venus as control. ON-TARGET plus SMART siRNA pool targeting mouse Rer1 (L-048547–01; Dharmacon) and ON-TARGET plus nontargeting pool (D-0010810-10) as control were transfected in C2C12 cells by using Amaxxa nucleofection. Up to 8×10^6 cells were nucleofected with 200 pmol siRNA in Nucleofector solution V by using program B-032.

Surface Labeling. For surface labeling of AChR, C2C12 cells were incubated with 200 nM αBT-biotin (Invitrogen) in PBS with 1 mM $CaCl_2$ and 0.5 mM $MgCl_2$ (PCM) for 30 min on ice. The binding of αBT-biotin to the assembled receptor was inhibited by preincubation with 2 mM carbachol (C4382; Sigma). Total surface proteins were labeled by incubating C2C12 cells with 0.5 mg/mL LC-sulfo-NHS-Biotin (Molecular BioSciences) in PCM for 30 min on ice. Cells were intensively washed either in PBS after αBT-biotin labeling or in 20 mM glycine in PBS after LC-sulfo-NHS-Biotin labeling and lysed in STEN lysis buffer (50 mM Tris at pH 7.6, 150 mM NaCl, 2 mM EDTA, 1% Nonidet P-40 and protease inhibitor mix). Streptavidin-agarose (Novagen) was used to recover biotinylated proteins. Quantitation of the Western blots was done by using chemiluminescence and a Fuji LAS4000 Luminescent Image Analyzer.

Immunoprecipitation and Immunoblotting. For immunoprecipitation, C2C12 cells were lysed in CHAPSO-lysis buffer (2% CHAPSO in 150 mM citrate buffer at pH 6.4 and protease inhibitor mix). Precleared lysates diluted to 1% CHAPSO concentration were incubated with 1 μg of the respective antibody for 3 h at 4 °C, then with Protein A- or G-Sepharose overnight at 4 °C. Beads were washed three times with 0.5% CHAPSO in 150 mM citrate buffer at pH 6.4 and once with 150 mM citrate buffer at pH 6.4 and boiled in Laemmli Buffer. When STEN lysates were used for IP, the beads were washed three times with 0.5% STEN buffer (50 mM Tris at pH 7.6, 150 mM NaCl, 2 mM EDTA, 0.5% Nonidet P-40) and once with STE buffer (STEN without Nonidet P-40). In some cases, Rer1 antibody was covalently coupled to Protein A-Sepharose.

Drug Treatments. Lysosomal and proteasomal degradation was blocked by overnight incubation with 20 μg/mL Leupeptin (Calbiochem) and for 4 h with 1 μM MG132 (Calbiochem), respectively.

Microscopy. β-Galactosidase staining was performed on muscle cryosections fixed in 0.1 M phosphate buffer at pH 7.4 containing 0.2% glutaraldehyde, 5 mM EGTA, and 2 mM $MgCl_2$ for 5 min at room temperature. After washing in 0.1 M phosphate buffer at pH 7.4, 0.01% Nonidet P-40, 0.02% Na-desoxycholate, 5 mM EGTA, and 2 mM $MgCl_2$, the sections were stained overnight in the same solution supplemented with 10 mM $K_3[Fe(CN)_6]$, 10 mM $K_4[Fe(CN)_6]$, and 0.5 mg/mL X-Gal. Adjacent sections were fixed in 2% PFA in PBS, and NMJs were stained overnight at 4 °C using αBT-AlexaFluor555 diluted 1:500 in PBS containing 1% BSA. Images were aquired on an Axio Imager by using a 20× 0.8 N.A. objective, a MRm camera and AxioVision software (all Carl Zeiss). In vivo confocal microscopy and microscopy of muscle sections was performed as described in ref. 22. Images were processed using Adobe Photoshop by following guidelines on figure preparation.

RT-PCR. Total RNA was isolated by using NucleoSpin RNAII kit (Macherey-Nagel). cDNA synthesized by using Transcriptor High Fidelity cDNA synthesis kit (Roche) was amplified for 25 cycles. For primer details, see *SI Materials and Methods*.

Gene Trap. Gene trap clone no. RPN 159 (Baygenomics) was used to create heterozygous mice by using standard protocols.

ACKNOWLEDGMENTS. We thank Veit Witzemann (Max-Planck-Institut für Molekulare Medizin Heidelberg) for cDNAs and helpful advice, the Fritz-Lipmann Institut and Institut für Toxikologie und Genetik animal facilities and Yvonne Petersen for excellent assistance; and Tiziana Cesetti, Jörg Stirnweiss, and Luchezar Karagyozov for critical comments on the manuscript. This work was supported by Deutsche Forschungsgemeinschaft Grants KA1751/2-1 (to C.K.) and RU923/4-1 (to R.R.).

1. Millar NS (2003) Assembly and subunit diversity of nicotinic acetylcholine receptors. *Biochem Soc Trans* 31:869–874.
2. Conti-Fine BM, Milani M, Kaminski HJ (2006) Myasthenia gravis: Past, present, and future. *J Clin Invest* 116:2843–2854.
3. Engel AG, et al. (1996) New mutations in acetylcholine receptor subunit genes reveal heterogeneity in the slow-channel congenital myasthenic syndrome. *Hum Mol Genet* 5:1217–1227.
4. Keller SH, Taylor P (1999) Determinants responsible for assembly of the nicotinic acetylcholine receptor. *J Gen Physiol* 113:171–176.
5. Millar NS, Harkness PC (2008) Assembly and trafficking of nicotinic acetylcholine receptors (Review). *Mol Membr Biol* 25:279–292.
6. Sato M, Sato K, Nakano A (2004) Endoplasmic reticulum quality control of unassembled iron transporter depends on Rer1p-mediated retrieval from the golgi. *Mol Biol Cell* 15:1417–1424.
7. Füllekrug J, et al. (1997) Human Rer1 is localized to the Golgi apparatus and complements the deletion of the homologous Rer1 protein of Saccharomyces cerevisiae. *Eur J Cell Biol* 74:31–40.
8. Kaether C, et al. (2007) Endoplasmic reticulum retention of the gamma-secretase complex component Pen2 by Rer1. *EMBO Rep* 8:743–748.
9. Spasic D, et al. (2007) Rer1p competes with APH-1 for binding to nicastrin and regulates gamma-secretase complex assembly in the early secretory pathway. *J Cell Biol* 176:629–640.

10. Bains W, Ponte P, Blau H, Kedes L (1984) Cardiac actin is the major actin gene product in skeletal muscle cell differentiation in vitro. *Mol Cell Biol* 4:1449–1453.
11. Sandonà D, Betto R (2009) Sarcoglycanopathies: Molecular pathogenesis and therapeutic prospects. *Expert Rev Mol Med* 11:e28.
12. Keller SH, Lindstrom J, Taylor P (1996) Involvement of the chaperone protein calnexin and the acetylcholine receptor beta-subunit in the assembly and cell surface expression of the receptor. *J Biol Chem* 271:22871–22877.
13. Christianson JC, Green WN (2004) Regulation of nicotinic receptor expression by the ubiquitin-proteasome system. *EMBO J* 23:4156–4165.
14. Hyman C, Froehner SC (1983) Degradation of acetylcholine receptors in muscle cells: Effect of leupeptin on turnover rate, intracellular pool sizes, and receptor properties. *J Cell Biol* 96:1316–1324.
15. Balice-Gordon RJ, Breedlove SM, Bernstein S, Lichtman JW (1990) Neuromuscular junctions shrink and expand as muscle fiber size is manipulated: In vivo observations in the androgen-sensitive bulbocavernosus muscle of mice. *J Neurosci* 10:2660–2671.
16. Wanamaker CP, Green WN (2007) Endoplasmic reticulum chaperones stabilize nicotinic receptor subunits and regulate receptor assembly. *J Biol Chem* 282:31113–31123.
17. Boulin T, et al. (2008) Eight genes are required for functional reconstitution of the Caenorhabditis elegans levamisole-sensitive acetylcholine receptor. *Proc Natl Acad Sci USA* 105:18590–18595.
18. Eimer S, et al. (2007) Regulation of nicotinic receptor trafficking by the transmembrane Golgi protein UNC-50. *EMBO J* 26:4313–4323.
19. Almedom RB, et al. (2009) An ER-resident membrane protein complex regulates nicotinic acetylcholine receptor subunit composition at the synapse. *EMBO J* 28:2636–2649.
20. Millar NS (2008) RIC-3: A nicotinic acetylcholine receptor chaperone. *Br J Pharmacol* 153(Suppl 1):S177–S183.
21. Rudolf R, Magalhães PJ, Pozzan T (2006) Direct in vivo monitoring of sarcoplasmic reticulum Ca2+ and cytosolic cAMP dynamics in mouse skeletal muscle. *J Cell Biol* 173: 187–193.
22. Röder IV, et al. (2008) Role of Myosin Va in the plasticity of the vertebrate neuromuscular junction in vivo. *PLoS ONE* 3:e3871.